Electrical Charge Transport and Optical Properties of a Poly(methacrylate) with a New Side Chain and Its Ni(II) Complex

F. Yakuphanoglu,[1] S. Sarman,[2] Y. Aydogdu,[1] Z. Ilter,[2] M. Coskun[2]

[1]*Department of Physics, Faculty of Arts and Sciences, Firat University, 23119 Elazig, Turkey*
[2]*Department of Chemistry, Faculty of Arts and Sciences, Firat University, 23119 Elazig, Turkey*

Received 29 January 2002; accepted 29 April 2002

ABSTRACT: The electronic conductivity of poly[2-(2-hydroxybenzyliden hydrazino)thiazole-4-yl methyl methacrylate] bearing a thiazole ring, Schiff base, and hydroxyl group in its side chain and its Ni(II) complex were measured as functions of temperature and frequency. The electrical measurements show the semiconducting nature of the samples as their electrical conductivity increased with increased temperature. Also, the activation energies were below 2 eV, which places them in the semiconductor regime. The conduction mechanism in the samples is discussed. Although extrinsic conduction mechanism occurs in the polymer, intrinsic conduction mechanism take places in its metal complex. The optical absorption spectra were recorded at room temperature and the optical energy gaps of samples were determined by optical spectra. © 2002 Wiley Periodicals, Inc. J Appl Polym Sci 87: 741–746, 2003

Key words: polymer; metal complex; conductivity; activation energy

INTRODUCTION

Organic semiconducting polymers constitute one of the most fascinating topics in chemistry and physics. There has been considerable interest in the synthesis and study of organic polymers, which may behave like metals or at least show high conductivities.[1,2] These compounds are interesting, from a scientific standpoint, concerning the study of fundamental problems of charge transfer. Of special interest are organic conducting and semiconducting polymers as a new class of electronic materials. They have attracted considerable attention because the investigation of these systems has generated entirely new scientific conceptions and a potential for its perspective application in molecular electronics. They contain an extended π electron system[3] that may be delocalized along the backbone, which can be switched from a semiconducting state to a conducting state.

A class of conducting polymers has an electronic structure, which consist of five-membered cyclic ring units with nitrogen or sulfur heteroatoms such as pyrole or thiophene. It is well known that conducting polymers contain π electrons, heteroatoms, and so forth, in their backbone.[4]

The materials that quality as organic semiconductors contain an appreciable number of carbon-carbon bonds representing of conjugation and exhibit electrical conductivity which varies exponentially with inverse of absolute temperature,[5]

$$\sigma = \sigma_0 \exp\left(-\frac{\Delta E}{kT}\right)$$

On the other hand, in the optical properties of polymers, the absorption process plays an important role. As is well known, for noncrystalline materials the classical zone theory is not valid. Polymers are type of materials. In this case, formation of the zone tails in the forbidden band and related equations are taken into consideration.[5] From the absorption spectra approximate absorption edges and optical activation energy can be calculated using the equation,

$$\alpha h\nu = A(h\nu - E_g)^r$$

In the present article we report the synthesis and characterization of poly[2-(2-hydroxybenzyliden hydrazino)thiazole-4-yl methyl methacrylate] bearing A thiazole ring, Schiff base, and hydroxyl group in its side chain, and the detailed experimental study of conductivity of this polymethacrylate with a new side chain and its metal complex.

Correspondence to: Y. Aydogdu (yaydogdu@firat.edu.tr).
Contract grant sponsor: Research Fund of Firat University; contract grant numbers: FUNAF-370, FUNAF-482.

Journal of Applied Polymer Science, Vol. 87, 741–746 (2003)

EXPERIMENTAL

Materials

1,3-Dichloroacetone and sodium methacrylate were purchased from Aldrich Chemical Co. and used without further purification. After it was dried with anhydrous MgSO4, acetonitrile (Merck) was distilled over P_2O_5 before use. 2,2-Azobisisobutyronitrile (AIBN; Merck) was used by recrystallizing from a mixture of ethanol and chloroform. *N,N*-dimethylformamide (DMF, Merck) was used as received. 2-Hydroxybenzylidene thiosemicarbazone was taken from Organic Chemistry Laboratory, where it was prepared for other purposes.

Preparation of 3-chloro-2-ketopropyl methacrylate

3-Chloro-2-ketopropyl methacrylate was synthesized by the reaction of 1,3-dichloroacetone and sodium methacrylate according to the method adapted from literature.[6]

For this purpose, 0.1 mol of 1,3-dichloroacetone, 0.1 mol of sodium methacrylate, a piece of each of NaI and hydroquinone, and 100 mL of dried acetonitrile were put into a three-necked flask and stirred at 70°C for 10 h. After it was extracted with diethyl ether, the product was dried over anhydrous MgSO4. 3-Chloro-2-ketopropyl methacrylate was distilled under vacuum (at 5 mmHg) at 130°C–132°C.

Characteristic FTIR bands: 1720 cm^{-1} (C═O stretching), 1646 cm^{-1} (C═C stretching), and 822 cm^{-1} (C—Cl stretching).

^{1}H-NMR (δ ppm): 1.97 (s, CH_3), 4.20 (s, CH_2Cl), 4.95 (s, OCH_2CO), and 5.69, 6.20 (═CH_2).

Preparation of 2-(2-hydroxybenzylidene hydrazino) thiazole-4-yl methyl methacrylate (BTMMA, the monomer)

According to the method given for the synthesis of a similar structure,[7] a mixture of 3-chloro-2-keto-propyl methacrylate (0.1 mol) and 2-hydroxybenzylidene thiosemicarbazone (0.1 mol) was refluxed in acetonitrile at 76°C for about 20 min in the presence of hydroquinone. The reaction content was poured into an aqueous solution of NH_3 (5%) and the precipitate (crude product) was filtered off and washed with water and dried. The crude product was dissolved in a hot mixture of ethyl acetate–ethanol (1:1 v/v), and the undissolved part was filtered off. The solution was allowed to crystallize the monomer, and the melting point of the solid monomer was 214°C.

Polymerization of the monomer

The polymerization of BTMMA was carried out in dioxane in the presence of AIBN as a radical initiator at 60°C for 48 h with a 75% conversion. Poly(BTMMA) was precipitated from methanol and dried under vacuum. Solveting in dioxane and precipitating from methanol was repeated for the polymer to purify it.

Preparation of the polymer–Ni(II) complex

A solution of 0.2 mmol of Ni(II)–acetate in water was added dropwise to a solution of 0.4 mmol (as a repeating unit) of poly(BTMMA) in 25 mL of dioxane, and the mixture was refluxed for 10 h. Then the reaction contents were poured into excess diethyl ether, and the polymer–Ni(II) complex precipitated was filtered off and washed with the ether and dried.

Sample preparation of electrical and optical measurements

Poly(BTMMA) and its Ni(II) complex were named as S1 and S2, respectively. Then these samples were pressed to make pellets about 0.1 cm thick at a pressure approximately 5×10^7 Pascal, and silver paint was applied by brushing at the two edges of the pellet to make electrical contacts. Electrical conductivities of the samples were measured by the two-probe method. The alternative current conductivities of the samples were measured as a function of frequency from 50 Hz to 9 kHz.

Instrumentation

IR analysis was performed using a Mattson 1000 FT-IR spectrometer. ^{1}H- and ^{13}C-NMR spectra were recorded on a Jeol FX-90Q spectrometer. DSC thermogram was obtained from a Shimadzu DSC-50 instrument at a rate of 20°C min^{-1}. Magnetic susceptibility was determined on Sherwood Scientific Magnetic Susceptibility Balance (Model MK1) at room temperature using $Hg[Co(SCN)_2]$ as a calibrant. The optical absorption spectra of the samples were taken from Perkin-Elmer Lambda 2S (double beam) spectrophotometer. Electrical conductivities of the samples were measured by using a Keithely 197/3A auto ranging multimeter and d.c and a.c source.

RESULTS AND DISCUSSION

Characterization studies

In the IR spectrum of the monomer, the most characteristic absorptions showed at 627 cm^{-1} (C—S—C in the thiazole ring), 1600 cm^{-1} (C═N in the thiazole ring and C═C in the aromatic ring), 1627 cm^{-1} (C═N azomethine), 1636 cm^{-1} (C═C olefinic), 1656 cm^{-1} (C═C in the thiazole ring), 1720 cm^{-1} (C═O in ester), 3050 cm^{-1} (═C—H in the aromatic ring and olefinic structure), and 3100–3200 cm^{-1} (O—H and N—H). In

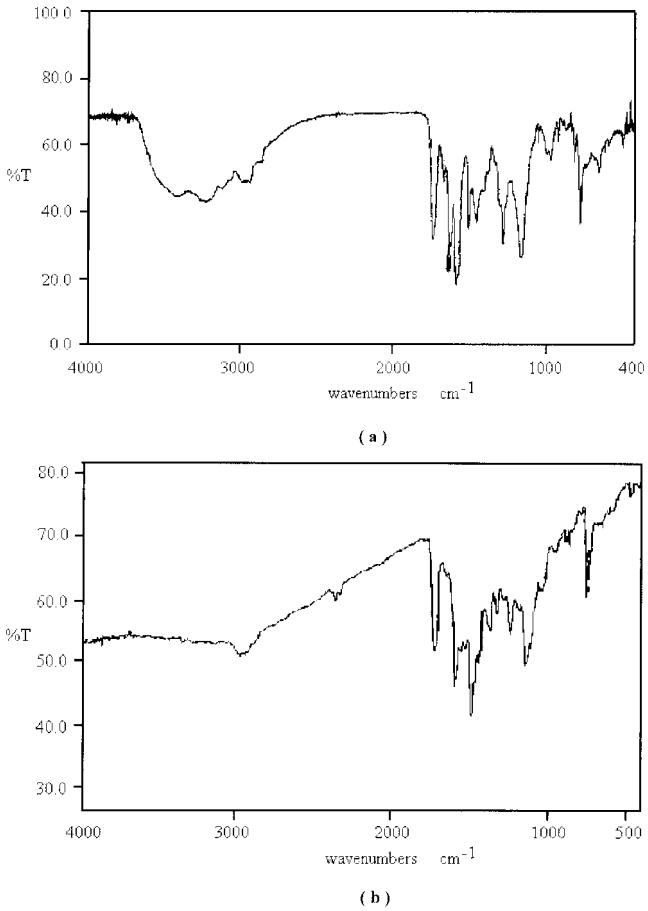

Figure 1 IR spectra: (a) poly(BHMMA) and (b) poly-(BHMMA)–Ni(II) complex.

the spectrum of the polymer [Fig. 1(a)], the C═O stretching shifted to 1735 cm^{-1}, the band at 1636 cm^{-1} of the monomer disappeared, and the O—H and N—H bands expanded to the 3200–3600 cm^{-1} range.

Characteristic ^{1}H-NMR peaks of poly (BTMMA) in the presence of d_6-DMSO and TMS, as solvent and internal standard were, respectively: 1.0 ppm (—CH_3), 2.2–2.4 ppm (—CH_2— in the polymer chain), 4.0–4.2 ppm (—$COOCH_2$—), 6.6–7.5 ppm (═CH—S in the thiazole ring and aromatic ring protons), 8.2 ppm (—N═CH— azomethine), 10.8 ppm (—OH on the aromatic ring), and 11.9 ppm (—NH-N═). ^{13}C-NMR spectrum of the polymer is shown in Figure 2, including the assignments according to carbon number in Scheme 1. The characteristic peaks in ^{13}C-NMR spectrum of the polymer ($CDCl_3$ and TMS, as solvent and internal standard, respectively) were: 177 ppm (C═O, C_4), 167 ppm (C═N in the thiazole ring, C_8), 157 ppm (CH═N azomethine, C_9), 146 ppm (HO—C in the phenyl ring, C_{11}), 142 ppm (quaternary carbon in C═CH—S in the thiazole ring, C_6), 129 ppm (C_{15} in the phenyl ring), 127 ppm (C_{13} in the phenyl ring), 119 ppm (C_7, ═CH in the thiazole ring), 118 ppm (C_{10} in the phenyl ring), 115 ppm (C_{14} in the phenyl ring), 106

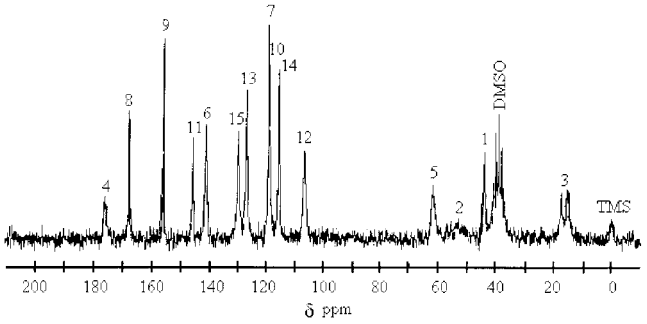

Figure 2 ^{13}C-NMR spectrum of poly(BHMMA). Solvent is DMSO-d_6.

ppm (C_{12} in the phenyl ring), 61 ppm (—OCH_2—,C_5), 50–54 ppm (quaternary carbon in polymeric backbone, C_2), 43 ppm (—CH_2—, C_1) and 15 and 17 ppm (CH_3, C_3, on the backbone). The bands at 3200–3600 cm^{-1} ranges of poly(BTMMA) disappeared in the IR spectrum [Fig. 1(b)] of its Ni(II) complex, and the band at 758 cm^{-1} (C—S stretching) shifted to 754 cm^{-1}.

Predicting from the DSC curve, poly(BTMMA) has a glass-transition temperature above 250°C. The magnetic susceptibility of its Ni(II) complex has been found to be 3.01×10^{-6} cgs, which means paramagnetic, and has a tetrahedral geometry in interchain coordination in which Ni bonds to oxygen on an aromatic ring and nitrogen with a double band in the side chain.

Electrical conductivity properties

The ac and dc conductivities of samples were measured, and the results can be interpreted as follows:

The ac electrical conductivities of samples are given in Figure 3, from which it is also evident that the dc contribution was significant at low frequencies, whereas the frequency-dependent term dominated at high frequencies. In these samples

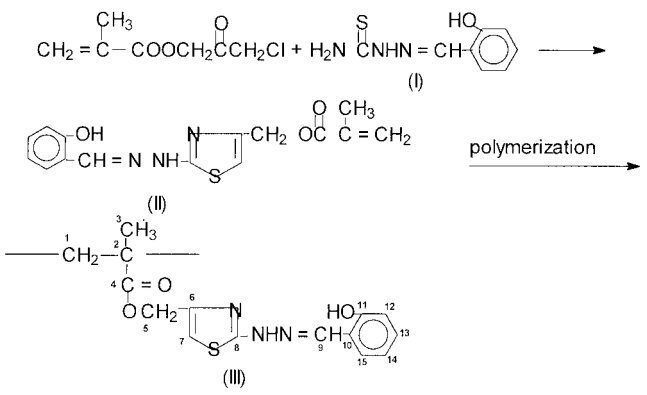

Scheme 1 The chemical structure of the monomer and polymer.

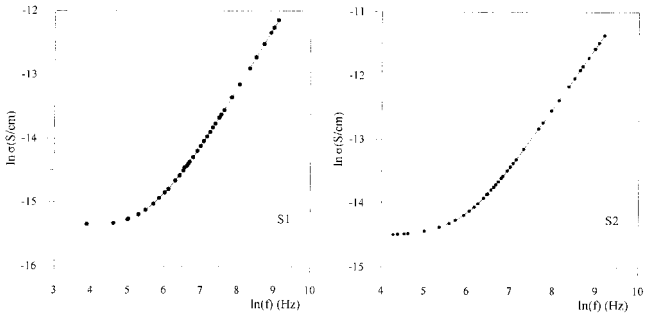

Figure 3 The relationship ln σ versus ln f for samples.

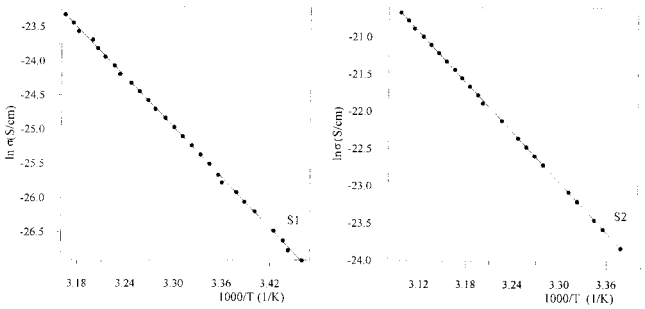

Figure 4 The relationship ln σ versus 1000/T for samples.

the total conductivity at a given frequency, ω, was considered as two components,[8]

$$\sigma(\omega) = \sigma_{dc} + A\omega^n \quad (1)$$

where σ_{dc} is the dc conductivity, A is a constant, and the parameter n is a frequency exponent with values between 0 and 1. It is evident from these curves that the ac conductivity had a frequency given by,

$$\sigma_{ac} \propto \omega^n \quad (2)$$

where the exponent n is a function of ω and o is $2\pi f$. We determined the n value from the slope of the graphs of log σ_{ac}–log f for the samples. To obtain the n value, we fitted the curves $\log_{ac}$–log f. The slope of curves was obtained from the equation,

$$n = \frac{d \log \sigma}{d \log f} \quad (3)$$

By applying a nonlinear, least-squares computer program, the results were fitted to eq. (2) in the high-frequency region. The calculated ac electrical parameters are given in Table I. The dependence of conductivity to frequency was detected as $\omega^{0.90-0.93}$ by fitting conductivity–frequency graphs of the samples shown in Figure 3. Two particular phenomena are seen in these plots. Starting at low frequency, the presence of a plateau followed by maximum of conductivity can be observed. The same shape of this spectrum is seen in two samples. Regarding this, the first and second evolutions correspond, respectively, to the hopping mode and vibrational mode.[9] The plateau characterizes the conduction, which is caused mainly by the hopping motion of the mobile electrons and determines the direct current value of conductivity. Thereafter, the slope of this plateau increased linearly with increasing frequencies.

TABLE I
Electronic Parameters of Samples

Parameter	S1	S2
ΔE (eV)	1.04	0.96
E_g (eV)	2.57	1.94
E_o (eV)	0.31	0.28
σ_{25} (S/cm)	6.72×0^{-12}	5.38×10^{-11}
σ_o (S/cm)	3.5×10^6	1.24×10^6
InA	−20.4323	−19.9624
n	0.90	0.93

Figure 4 shows temperature dependence of conductivity, which was examined according to the Arrhenius theory. Electrical conductivity, σ, of the samples follows the Arrhenius type equation:

$$\sigma = \sigma_0 \exp\left(-\frac{\Delta E}{kT}\right) \quad (4)$$

where ΔE is the activation energy for electron transfer, σ_o is the preexponential corresponding to $1/T = 0$, and k is the Boltzmann constant. The electrical conductivity graphs of samples are presented in Figure 4. It appears that σ follows eq. (4) over the complete temperature range. It is well known that in disordered materials, charge transport mechanism must be considered: transport by carriers excited beyond a mobility edge into the extended states E_C (conduction band edge) or E_V (valence band edge) leading to an activated energy $\Delta E = E_C$–E_F or $(E_F - E_V)$ at high temperatures and the hopping of carriers between localized states in the gap at lower temperatures.[5] The activation energy, ΔE, was calculated from the slope of the straight line, and the preexponential factor, σ_o, was obtained by extrapolating the ln σ line to the value corresponding to $1/T = 0$. The obtained values are given in Table I. The calculated value of ΔE alone does not provide any indication of whether the conduction occurred in the extended states above the mobility edge or by hopping in the localized states.[5] According to Mott[5,10] values of σ_o are in the range 10^3–10^4 (S/cm) in the extended states. A smaller value of σ_o indicates the presence of wide localization and conduction by hopping in the localized state. The calculated values for samples, both ΔE and σ_o, suggest that electrical conduction takes place in extended states. The activation energy values are shown in Table I. If the conventional band–type conduction mechanism is appli-

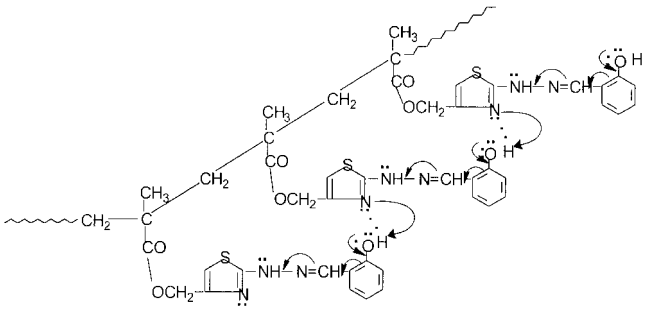

Scheme 2 Intramolecular charge transfer from one unit to its adjacent one.

cable to these samples, $2\Delta E$ should correspond to the band gap energy. The electrical measurements for these samples show that the conductivity obeys Eq. (4), which would suggest that conduction might occur by an intrinsic band model because optical absorption starts at about $2\Delta E$.[11] It can be seen from Table I that the optical absorption for the S2 sample starts at about $2\Delta E$. But it does not start in S1 sample. It is suggested that although intrinsic conduction occurs in the S2 sample, in the S1 sample extrinsic conduction takes place. In intrinsic conduction activation of charge carriers is from the valence band to the conduction band. But ΔE corresponds to the distance between the donor level and the conduction band edge for n-type extrinsic conduction or corresponds to the distance between the acceptor level and the valence band edge for p-type extrinsic conduction. The conduction type of the polymer was determined by hot probe and found to be p-type conduction. So, in S1 sample activation was from the valence band to the acceptor level. As the S1 sample shows, semiconducting behavior in organic polymeric semiconductors has two stages in the movement of current carrier motion within the macromolecule and passage from one macromolecule to another, that is, the intramolecular and intermolecular transfer of the current carrier. It is considered that the intramolecular conduction process occurs in polymer (S1), as shown in Scheme 2. This conduction mechanism can be explained as follows: in the side chain of this poly(methacrylate), there are several π bonds and electron pair donors such as nitrogen and oxygen atoms. A resonance stabilization begun by moving of an unshared electron pair on an oxygen atom to benzene ring causes the temporary location between two nitrogen atoms of π electrons shared by nitrogen and carbon. Although a polymeric main chain does not have any structure causing electrical conductivity, this delocalization of electrons extends present conjugation in the side chain of the polymer from nitrogen in the thiazole ring to an oxygen atom on the benzene ring. After the removal of π electrons, the nonbonding electron pairs require lower energy and finally conjugation extends them, making this phenomena possible. The conjugated double bonds create a decrease in the system's internal energy and apparently allow electron transfer for electronic conduction. So, conjugation may be enough to make the polymer material semiconducting[13] if it were to be present throughout a main chain. All these events occurring on the side chain of one unit are not sufficient to explain electrical conductivity of this polymer without the presence of charge transporter from one unit to other. On the other hand, hydrogen bonds between a hydrogen atom bonded to a oxygen atom and nonbonding electron pair on a nitrogen atom in a thiazole ring in the side chain of neighboring unit may ensure charge transfer from one unit to its adjacent one (Scheme 2).

As the conductivities of samples were compared with each other, it was found that the conductivity of the S2 sample was higher than that of S1. This can be explained as follows: The introduction of a metal with an organic polymer generally increases its conductivity. The metal provides additional conductivity by virtue of its own electronic characteristics, which means that d electrons available in the metal atom play an important role in the polymer.[14,15] Also, the increase of conductivity is considered a result of the interaction between the metal atom and the ligand because this interaction can be alleviated by transfer of electrons in the complex structure.

Optical properties

To obtain energy-band gaps of the samples, the optical spectra were recorded at room temperature. The results are given in Figure 5. The optical-band gaps of samples were determined by applying the relation,[5,16]

$$\alpha h\nu = A(h\nu - E_g)^r \tag{5}$$

where $h\alpha$ is the photon energy, E_g is the optical energy gap of the material, and the exponent r takes values of 1, 2, 3, or ½, depending on the types of electronic transition in the k space. We evaluated E_g from optical absorption spectra of the samples for photon energy larger than 1.8 eV. The best fitting to the absorption spectra in eq. (5) gave $r = ½$, meaning it allowed direct transition for these samples.

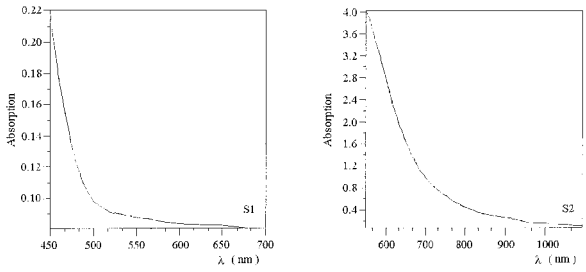

Figure 5 Absorption spectra for samples.

Figure 6 shows plots of $(\alpha h\nu)^2$ versus $(h\nu)$ for samples. The extrapolation of the linear relationship between $(\alpha h\nu)^2$ and $(h\nu)$ to $(\alpha h\nu)^2 = 0$ gives E_g, as shown in Figure 6.

On the contrary, the relation between the absorption coefficient, α, and the photon energy, $h\nu$, is given according to the well-known Urbach rule,[5,17]

$$\alpha = \alpha_0 \exp\left[\frac{\gamma(h\nu - E_g)}{kT}\right] \quad (6)$$

where ν is the frequency of radiation, k is the Boltzmann constant, and α_0 is a constant. γ/kT gives a measure of the steepness of the absorption edge and is sometimes interpreted as the width of the tail of localized states in the band gap. The Urbach relation at a particular temperature could be reduced to,

$$\alpha = \alpha_0 \exp(h\nu/E_0) \quad (7)$$

where α_0 and E_0 are material-dependent constants and E_0 is interpreted as the width of tails of localized states in the band-gap region. The linear dependence of ln α versus $h\nu$ is presented in Figure 7 according eq. (7). The slope of the curves gives the width of the band tail, E_0, as explained above. Table I summarizes the obtained data.

CONCLUSIONS

It was found that the polymer bearing the thiazole ring, Schiff base, phenyl ring, and hydroxyl group in its side chain and its Ni(II) complex have an organic semiconducting property with moderately activation energy and conductivity values. The optical absorption measurements indicated that these samples have a direct optical-band gap.

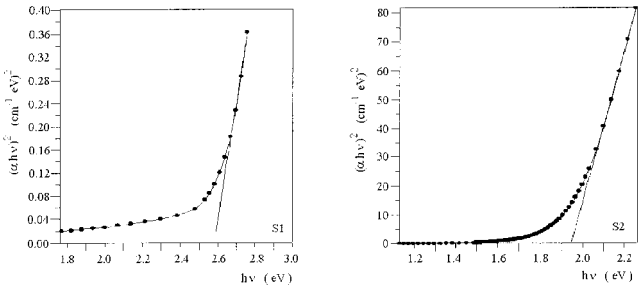

Figure 6 The plots of $(\alpha h\nu)^2$ versus $h\nu$ for samples.

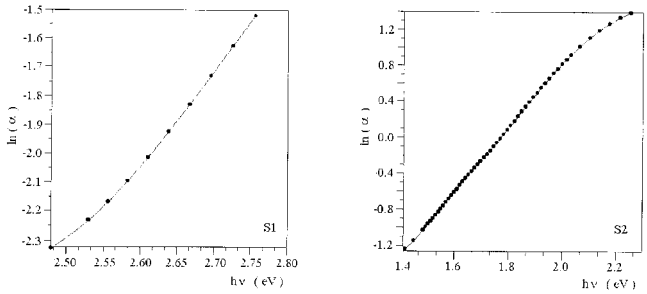

Figure 7 Variation of the ln α versus hν for samples.

The support of the Research Fund of Firat University under research Projects Nos. 370 and 482 (FUNAF-370 and FUNAF-482) is gratefully acknowledged.

References

1. Shirakawa, H.; Ikeda, S. Polym J 1971, 2, 231.
2. Shirakawa, H.; Ikeda, S. Polym J 1973, 4, 460.
3. Wang, Z. G.; Ray, A.; MacDiamid, A. G.; Epstein, A. J. Phys, Rev B 1991, 43, 4373.
4. Kaynak, A. Mat Res Bull 1998, 33, 81.
5. Mott, N. F.; Davis, E. A. Electronic Processes in Non-crystalline Materials; Clarendon Press: Oxford, England, 1971.
6. Joncky, A.; Kmiotek-Skarzynskaad, I.; Zdrojewski, T. J Chem Soc, Perkin Trans 1994, 1, 1605.
7. Cukurovali, A.; Yilmaz, I.; Ozmen, H. Transition Met Chem 2001, 26, 619.
8. Bhattacharyya, S.; Saha, S. K.; Chakravorty, M.; Mandal, B. M.; Chakravorty, D.; Goswami, K. J Polym Sci, Part B: Polym Phys 2001, 39, 1935.
9. Benmoussa, H.; Mikou, M.; Bensaoud, A.; Bouhanouss, A.; Morineaux, R. Mat Res Bull 2000, 35, 369.
10. Mott, N. F.; Davis, E. A. Electronic Processes in Non-crystalline Materials, Clarendon Press: Oxford, England, 1979.
11. Aydogdu, Y.; Yakuphanoglu, F.; Aydogdu, A.; Temel, H.; Sekerci, M.; Hosgoren, H. Sol State Sci 2001, 3, 377.
12. Kao, K. C.; Hang, W. Electrical Transport in Solids: Pergamon Press: Germany, 1981.
13. Okamoto, Y.; Brenner, W. Organic Semiconductors, Reinhold Publishing Corporation; Chapman & Hall: London 1964.
14. Samuelson, A. G.; Alagesan, K. Synth Met 1997, 87, 37.
15. Aydogdu, Y.; Yakuphanoglu, F.; Aydogdu, A.; Sekerci, M.; Balci, Y.; Aksoy, I. Synth Met 1999, 107, 191.
16. Taue, J. Amorphous and Liquid Semiconductors; Plenum Press: London, 1976; Chapter 6.
17. Bahgat, A. A.; El-Samanoudy, M. M.; Sabry, A. I. J Phys Chem Solids 1999, 60, 1921.